

## Spin Exchange Coupling in Dimethoxy-Bridged Dichromium(III) Complexes: A Density Functional Theory Study

Dae-Bok Kang

Department of Chemistry, Kyungsung University, Busan 608-736, Korea. E-mail: dbkang@ks.ac.kr

Received January 13, 2008

For the  $[\text{Cr}_2(\text{H}_2\text{tmp})_2\text{Cl}_4]$  compound, simplified models with two bridging methoxy ligands have been studied. The influence of the bridging Cr-O-Cr bond angles on the exchange coupling between metal atoms in the model compound has been analyzed by means of density functional calculations with the broken-symmetry approach. Coupling constant calculated for the full structure is in good agreement with the experimentally reported value, confirming the validity of the computational strategy used in this work to predict the exchange coupling in a family of related dinuclear Cr(III) compounds. The calculations indicate a good correlation between the calculated coupling constant and the sum of the squared energy gap of three pairs of metal  $t_{2g}$  OMSOs with a limited variation of the Cr-O-Cr angle. The spin density distribution and the mechanism of magnetic coupling interactions are discussed.

**Key Words :** Exchange coupling, Density functional theory, Magneto-structural correlation

### Introduction

The exchange interactions between the molecular fragments carrying a localized spin has been of considerable interest in the field of theory of magnetism. This interest has also been greatly spurred by the search for the spin arrangements of single molecular magnets in which the magnetic coupling occurs between transition metal ions in a complex with various ligand environments.<sup>1,2</sup> Recently, the broken-symmetry density functional theory (BS-DFT) approach<sup>3</sup> has been mostly used for investigations of magnetic exchange coupling constants ( $J$ ) in dinuclear and polynuclear transition-metal complexes because these methods have proven to give good numerical estimates of  $J$  values.<sup>4</sup>

We have studied the exchange coupling in methoxy-bridged Cr(III) compounds by analyzing the influence of the specific change in the  $[\text{Cr}(\mu\text{-OCH}_3)_2\text{Cr}]^{4+}$  core geometry on the coupling constant. Unlike the electronically simple copper(II) dimers having only one unpaired electron localized on each metal center, the chromium(III) dimers in which each  $\text{Cr}^{3+}$  ion bears three unpaired d electrons present an ideal example for the study of the structure-magnetism relations. In this study, we have calculated  $J$  values on the full size and simplified model compounds shown in Figure 1 by using the BS-DFT approach and examined the magneto-structural correlations for Cr-O-Cr angle distortions found in this system.

### Computational Details

Since the computational methodology adopted in this work has been described in detail elsewhere,<sup>5</sup> it will be only briefly reviewed here. Assuming the Heisenberg spin Hamiltonian is defined as  $H = -JS_1 \cdot S_2$  to describe the exchange coupling in a dinuclear compound, where  $J$  is the coupling constant, and  $S_1$  and  $S_2$  the local spins on centers 1 and 2,

respectively, the coupling constant  $J$  can be evaluated from the calculated energies of the high-spin and broken-symmetry states according to the following expression:

$$J = \frac{2(E_{\text{BS}} - E_{\text{HS}})}{S(S+1)} \quad (1)$$

where  $S$  is the total spin for the high-spin state and  $E_{\text{BS}}$  and  $E_{\text{HS}}$  are the calculated energies for the broken-symmetry (BS) and high-spin (HS) states, respectively. The broken-symmetry approach has been employed to describe the unrestricted solutions of the antiferromagnetic singlet spin states.

The hybrid B3LYP method<sup>6</sup> has been used in all calculations as implemented in Gaussian03 program,<sup>7</sup> mixing the exact Hartree-Fock exchange with Becke's expression for the exchange functional<sup>8</sup> and using the Lee-Yang-Parr correlation functional.<sup>9</sup> Double- $\zeta$  quality basis sets<sup>10</sup> have been employed for all atoms except for the Cr atom, for which a triple- $\zeta$  basis set<sup>11</sup> with two extra p orbitals (polarization functions) has been used. No molecular optimization has been done, with the full experimental geometry of the dimeric complex used for the calculations. Throughout the calculations all bond lengths were fixed. We systematically varied the Cr-O-Cr bridging angle in the model complex, keeping all other angles constant at the values in the full structure.

### Structure Description

The geometry of the dimeric complex  $[\text{Cr}_2(\text{H}_2\text{tmp})_2\text{Cl}_4]$  (Figure 1a) was obtained from X-ray crystallographic data.<sup>12</sup> The positions of the hydrogen atoms are available in the crystal structure data. We use the notation of  $\text{H}_2\text{tmp}$  for the tripodal ligand 1,1,1-tris(hydroxymethyl)propane. Selected bond lengths and angles are given in Table 1. The structure consists of two Cr(III) ions linked by two singly deproto-

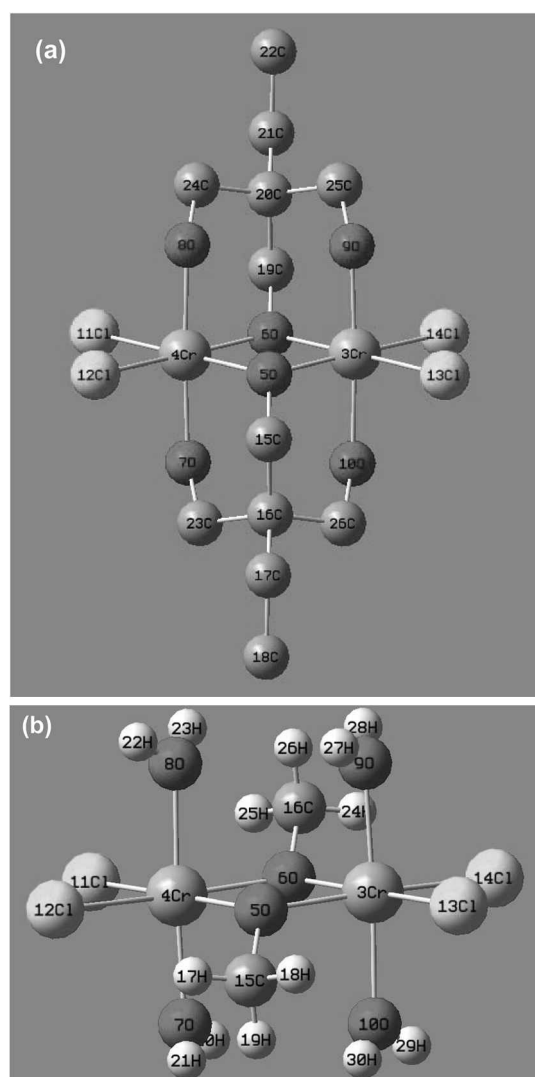


**Figure 1.** (a)  $[\text{Cr}_2(\text{H}_2\text{tmp})_2\text{Cl}_4]$  compound and (b) the simplified model of the compound.

**Table 1.** Selected interatomic distances (Å) and angles ( $^\circ$ ) for  $\text{Cr}_2(\text{H}_2\text{tmp})_2\text{Cl}_4$  compound

Cr4-O5	1.964	Cr4-Cl11	2.338
Cr4-O6	1.954	Cr4-Cl12	2.309
Cr4-O7	1.983	Cr4-Cr3	3.022
Cr4-O8	2.017		
Cr4-O5-Cr3	100.9	O5-Cr4-Cl12	93.5
O5-Cr4-O6	79.1	O6-Cr4-Cl11	94.4
O5-Cr4-O7	87.8	O6-Cr4-Cl12	171.8
O6-Cr4-O7	90.6	O7-Cr4-Cl11	90.0
O5-Cr4-O8	90.5	O7-Cr4-Cl12	92.6
O6-Cr4-O8	86.9	O8-Cr4-Cl11	91.4
O7-Cr4-O8	177.2	O8-Cr4-Cl12	89.7
O5-Cr4-Cl11	173.1	Cl11-Cr4-Cl12	93.2

nated  $\text{H}_2\text{tmp}^-$  ligands, being related by an inversion center. The deprotonated arms (O5 and O6) act as  $\mu$ -bridges with the protonated arms (O7-O10) bound to metal ions in a terminal fashion. The axial oxygen bonds to Cr in the latter

bridges are slightly longer [1.983-2.017 Å] than the bridging Cr-O distances [1.954-1.964 Å] in the former which reveal Cr3-O5 and Cr4-O5 to be unequal, also Cr3-O6 and Cr4-O6 to be unequal. Two terminal chloride ions (Cl11, Cl12 and symmetry equivalents) complete the coordination spheres of the Cr(III) ions and are almost coplanar with the  $\text{Cr}_2\text{O}_2$  motif. The Cr(III) ions are in distorted octahedral geometries with *cis* angles in the range 79.1-94.4 $^\circ$  and *trans* angles of 171.8-177.2 $^\circ$ .

Apart from building full size structure for the above compound, we also created simplified model structures of it in order to investigate the possibility to employ only rudimentary ligand structures instead of full size ligands in the calculations of exchange coupling constants as this would allow for a significant reduction of the computational cost. The model compound was designed by replacing the large ligands encountered in the dichromium complex with suitable smaller ligands such as  $\text{H}_2\text{O}$  and  $\text{OCH}_3$ , as shown in Figure 1b. The positions of heavy atoms (C, O, Cl, Cr) have been selected to be the same as in the full size structure.

## Results and Discussion

The results of the calculations of the exchange coupling constants between Cr(III) centers in the dinuclear chromium complex along with available experimental data are summarized in Table 2. An exchange coupling constant,  $J = -7.5 \text{ cm}^{-1}$ , has been obtained from calculations on the full size complex in which the metal ions present distorted octahedral coordination environments (Figure 1a). We have used in our calculations the molecular structure as determined experimentally by X-ray diffraction rather than an optimized one, since small changes with respect to the experimental structure could result in significant deviations of the calculated coupling constant. The calculated  $J$  value is in a fairly good agreement with the experimental value. It is evident that there is a weak antiferromagnetic superexchange interaction between the two chromium(III) centers in the dimer complex. After verifying the agreement between calculated values of  $J$  for the full size and the model structure, we analyze the dependence of the exchange coupling on the Cr-O-Cr bridging angle by performing calculations on the model system  $[\text{Cr}_2(\text{OCH}_3)_2(\text{H}_2\text{O})_4\text{Cl}_4]$  built from the experimental structural parameters of  $[\text{Cr}_2(\text{H}_2\text{tmp})_2\text{Cl}_4]$  (Figure 1b), then the magneto-structural correlations for bridging angle distortions expected in this family of compounds.

**Influence of the Cr-O-Cr bridging angle on the exchange coupling.** We have found in Table 2 that the difference between the coupling constants computed employing

**Table 2.** Calculated and experimental coupling constants for full and model structures of  $\text{Cr}_2(\text{H}_2\text{tmp})_2\text{Cl}_4$  compound

Structure	$J_{\text{calcd}} (\text{cm}^{-1})$	$J_{\text{exp}} (\text{cm}^{-1})^a$
full	-7.5	-12.3
model	-8.5	

<sup>a</sup>From ref 12.

**Table 3.** Calculated coupling constants for methoxy-bridged model structures presenting different Cr-O-Cr angles ( $^{\circ}$ ) and Cr...Cr distances ( $\text{\AA}$ ); the relative energy (kcal/mol) of the broken-symmetry (BS) and high-spin (HS) states is also included

Cr-O-Cr	Cr...Cr	$-J(\text{cm}^{-1})$	$E_{\text{rel}}$ (BS)	$E_{\text{rel}}$ (HS)
106.9	3.15	18.0	2.3	2.5
100.9	3.02	8.5	0.0	0.0
94.9	2.89	37.5	3.5	4.0
88.9	2.74	141.8	12.5	14.8
82.8	2.59	369.7	27.9	34.1

the full size structure and its simplified model geometry is small, with the deviation of  $1 \text{ cm}^{-1}$ . Therefore, it is possible to use simplified model structures of the dinuclear chromium complex without affecting the magnetic coupling between the Cr(III) centers. The success of this methodology indicates that only the closest environment of the Cr(III) centers have significant effects on their electronic structure due to a localized nature of the unpaired electron orbitals.

For the geometrical arrangement of the  $[\text{Cr}(\mu\text{-OCH}_3)_2\text{-Cr}]^{4+}$  core in the model complex consisting of two edge-sharing octahedrally coordinated Cr(III) centers only the Cr-O-Cr angle ( $\varphi$ ) has been varied between  $82^{\circ}$  and  $107^{\circ}$  with the other structural parameters unchanged. The calculated coupling constant  $J$  and the relative energy of each geometry are shown in Table 3. It is important to note that the minimum energy for each of the broken-symmetry and high-spin states corresponds to a Cr-O-Cr angle of *ca.*  $101^{\circ}$ . Figure 2a shows a plot of the energies of both spin states as a function of  $\varphi$  with a minimum at  $\varphi = 101^{\circ}$ , in excellent agreement with the experimental structure.

Hodgson showed that there exists a magneto-structural correlation for several compounds displaying the  $[\text{Cr}_2(\text{OR})_2]^{4+}$  core ( $\text{R} = \text{H}, \text{CH}_3$ ), which relates the magnetic coupling constant to some structural factors such as the Cr-O-Cr angle, the Cr-O distance, and the dihedral angle formed by the OR group and  $\text{Cr}_2\text{O}_2$  plane.<sup>13</sup> Although the magnitude of exchange coupling strongly depends on each of these factors, we analyze the dependence of the coupling constant on the Cr-O-Cr angle (or the Cr...Cr distance, since the Cr-O distance has been kept frozen). The calculated  $J$  values are represented in Figure 2b as a function of  $\varphi$ . The calculated coupling constant exhibits a significant variation with Cr-O-Cr angle, becoming more negative (*i.e.*, enhanced antiferromagnetic coupling) for small values of the Cr-O-Cr bridging angle ( $\varphi < 95^{\circ}$ ) and correspondingly Cr...Cr distances short enough to allow direct interaction between the paramagnetic centers as a consequence of the increased through-space overlap between the  $x^2-y^2$  metal orbitals. This strong antiferromagnetic coupling drops sharply and becomes weakly antiferromagnetic at Cr-O-Cr angles close to  $100.9^{\circ}$  slightly distorted from the real molecule, reaching a minimum at about  $101^{\circ}$ . The dependence of the exchange coupling constants  $J$  on the Cr-O-Cr angle in model complexes indicates that the spin exchange interaction between the Cr(III) magnetic centers is quite sensitive to the variation

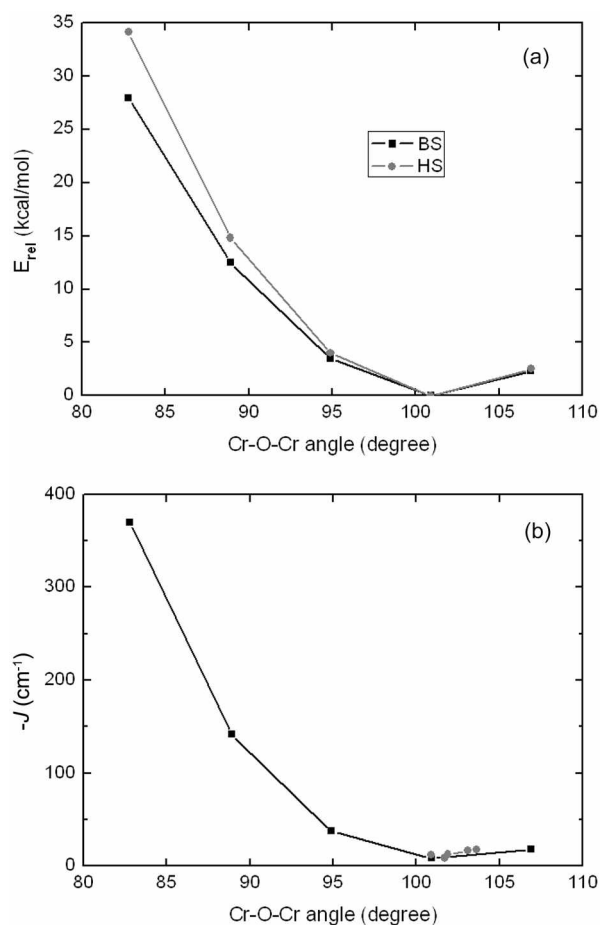


**Figure 2.** (a) Relative energy of the broken-symmetry (squares) and high-symmetry (circles) states as a function of the Cr-O-Cr bridging angle; (b) variation of the calculated coupling constant  $J$  (squares) as a function of the Cr-O-Cr bridging angle for the model compound, together with experimental values (circles).<sup>(12,18,21)</sup>

of the bridging angle.

The general behavior of the experimental data for dinuclear complexes (Figure 2b, closed circles) seems to be in agreement with the calculated values for the model compound, although the limited number of experimental data precludes at the present time a full verification of the predicted dependence of  $J$  on the bridging angle. Structures with Cr-O-Cr angles ranging from  $95^{\circ}$  to  $107^{\circ}$  are possible from the energetic point of view for each of the three configurations studied (Table 3), since only energy less than 5 kcal/mol is needed to produce such a distortion. This result is in good agreement with the fact that experimental structures present Cr-O-Cr angles within this range of values.

**Qualitative orbital model.** The aforementioned magneto-structural correlation has also been analyzed by means of the qualitative molecular orbital model proposed by Hoffmann and co-workers<sup>14</sup> in order to find the electronic factors that govern it. According to the theoretical analysis presented by these authors, in a dinuclear complex with two unpaired electrons described by the singly occupied molecular orbitals (SOMOs), the coupling constant expressed as the singlet-triplet energy separation ( $J$ ) can be approximated by eq. (2).

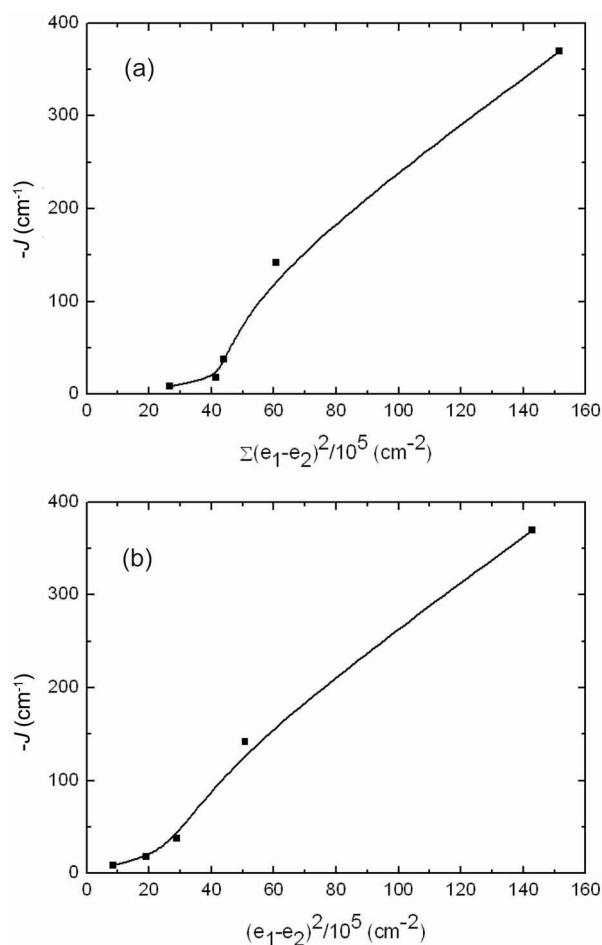
**Table 4.** Calculated energy gap squares ( $\text{cm}^{-2}$ ) between the symmetric and antisymmetric combinations of the  $t_{2g}$  and  $x^2-y^2$  orbitals

Cr-O-Cr (deg)	$-J$ ( $\text{cm}^{-1}$ )	$\Sigma(e_1-e_2)^2/10^5$ ( $t_{2g}$ )	$(e_1-e_2)^2/10^5$ ( $x^2-y^2$ )
106.9	18.0	41.4	19.1
100.9	8.5	26.6	8.5
94.9	37.5	43.9	28.8
88.9	141.8	60.6	50.8
82.8	369.7	151.5	142.8

$$E_S - E_T = J = 2K_{ab} - \frac{(e_1 - e_2)^2}{J_{aa} - J_{ab}} \quad (2)$$

Here,  $e_1$  and  $e_2$  are the SOMO energies of the complex in the triplet state,  $K_{ab}$  is the exchange integral between the magnetic orbitals a and b representing the two spin sites, and  $J_{aa}$  and  $J_{ab}$  are the corresponding Coulomb integrals. The first term ( $2K_{ab}$ ) is positive and can be considered the ferromagnetic contribution to the exchange coupling, responsible for the stability of the triplet state, whereas the second term is negative and represents the antiferromagnetic contribution favoring the singlet state. Only when the second term is zero or negligible, the ferromagnetic behavior is predominant. The antiferromagnetic contribution to the coupling constant should be proportional to the square of the energy gap,  $(e_1 - e_2)^2$ , of pairwise MO's derived from the magnetic orbitals. Assuming that the two-electron terms ( $K_{ab}$ ,  $J_{aa}$ , and  $J_{ab}$ ) are approximately constant for a given magnetic system, changes in the coupling constant are usually interpreted as reflecting the variations in the energy difference between the pairwise MO's bearing the unpaired electrons.<sup>15</sup>

For the present case of three spins per spin site, it can be seen that the linear relation predicted by Hoffmann and co-workers holds for the dimethoxy-bridged dinuclear Cr(III) models studied here if the occupied magnetic spin-orbitals (OMSOs) in the high-spin state<sup>16</sup> are considered. As in the case with one unpaired electron, a practically linear correlation exists between the calculated  $J$  and the sum of the squares of the orbital energy gap in the high-spin state (see Figure 3a). Usually, the antiferromagnetic contributions to the exchange coupling from the crossed terms involving different magnetic orbitals in each metal ion are considered negligible with respect to the stronger antiferromagnetic contributions.<sup>17</sup> When the magnetic orbitals are different in symmetry and shape, the overlap between them is zero or negligibly small. In octahedral Cr(III) systems the three unpaired electrons are occupying the  $t_{2g}$  orbitals. We have thus considered only three contributions that are related to the energy gap of the pairs of OMSOs that contain the symmetric and antisymmetric combinations of the three  $t_{2g}$  magnetic orbitals of each metal ion in the model compound. The calculated gaps are presented in Table 4. The result shows that the antiferromagnetic terms can be traced to the separate contributions of the  $x^2-y^2$  and the other two orbitals. The larger gap can be attributed to the more favorable  $t_{2g}$ -

**Figure 3.** Dependence of the coupling constant  $J$  on (a) the sum of squared energy gap of three pairs of metal  $t_{2g}$  OMSOs and (b) the square of the energy gap between the pairwise  $x^2-y^2$  OMSOs for model compounds at different values of the Cr-O-Cr bridging angle.

bridging ligand overlap, which should result in a stronger antiferromagnetic coupling. The largest contribution comes from the  $x^2-y^2$  magnetic orbitals. Since the  $x^2-y^2$  orbitals are not pointing directly at the bridging ligands, but to the other metal center, the  $\sigma$  overlap between the  $x^2-y^2$  metal orbitals favors a direct through-space exchange mechanism (Figure 4), becoming larger when the Cr-O-Cr angle and the Cr...Cr distance decrease. The contributions from the  $xz$  and  $yz$  magnetic orbitals are not significant. It is noteworthy that there is also a good linear correlation between the calculated  $J$  values and the squared energy gap of a pairs of the ( $x^2-y^2$ )-like OMSOs, except for the very small gaps that result for slightly distorted arrangements of the Cr-O-Cr backbone near  $\varphi = 100.9^\circ$  (Figure 3b). Such results indicate that the structural dependence of the exchange coupling in the presently studied Cr(III) complexes is practically governed by the energy split of the pairwise  $x^2-y^2$  OMSOs.

**Spin population analysis.** In order to explore the magnetic exchange mechanism in the Cr(III) dimers, the net spin populations reduced on individual atoms are analyzed. The spin populations calculated for the high-spin (HS) and

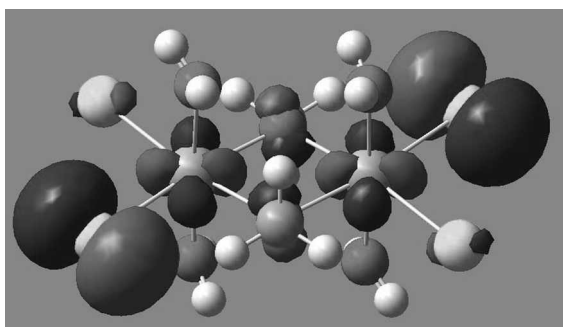


Figure 4. Calculated ( $x^2-y^2$ )-like OMSOs of the high-spin state for the model compound.

Table 5. Mulliken atomic spin populations calculated for the high-spin (HS) and the broken-symmetry (BS) states of the full structure (Figure 1a)

Atom	HS	BS
Cr(3)	2.9638	2.9562
Cr(4)	2.9638	-2.9562
O(5)	0.0073	0.0039
O(6)	0.0073	-0.0039
O(7)	-0.0080	0.0076
O(8)	-0.0084	0.0082
O(9)	-0.0080	-0.0076
O(10)	-0.0084	-0.0082
Cl(11)	0.0125	-0.0109
Cl(12)	0.0209	-0.0195
Cl(13)	0.0125	0.0109
Cl(14)	0.0209	0.0195
C(15)	0.0057	0.0001
C(19)	0.0057	-0.0001
C(23)	0.0007	-0.0001
C(24)	0.0007	-0.0003
C(25)	0.0007	0.0001
C(26)	0.0007	0.0003

broken-symmetry (BS) states of the full structure are listed in Table 5. The plus and minus signs indicate  $\alpha$  and  $\beta$  spin states, respectively. In the HS state, the spin populations on Cr atoms are 2.9638 while the spin populations on other atoms are all very small, demonstrating the delocalization of a small part of spin densities from Cr atoms to peripheral atoms. The equatorial atoms around Cr-including O(5), O(6), Cl(11), Cl(12), Cl(13), and Cl(14)-have small positive spin populations, suggesting a predominant effect of the spin delocalization from Cr(3) and Cr(4). In contrast, for the axially coordinating ligand bridges around Cr, the spin polarization from the Cr centers leads to negative spin populations on O(7), O(8), O(9), and O(10).

On the other hand, in the BS state Cr(3) and Cr(4) have opposite spin populations. The O(9) and O(10) atoms have  $\beta$  spin populations due to the spin polarization of Cr(3) with  $\alpha$  spin population, while the O(7) and O(8) atoms have  $\alpha$  spin populations due to the spin polarization of Cr(4) with  $\beta$  spin population. However, the bridging atoms O(5) and O(6) indicate the spin delocalization from the magnetic centers

Table 6. Mulliken atomic spin populations calculated for the high-spin state of model structures (Figure 1b) at different values of the Cr-O-Cr bridging angle

Atom	Cr-O-Cr bridging angle (deg)				
	106.9	100.9	94.9	88.9	82.8
Cr(3)	2.9582	2.9555	2.9510	2.9448	2.9370
Cr(4)	2.9582	2.9555	2.9510	2.9448	2.9370
O(5)	0.0060	0.0103	0.0170	0.0258	0.0360
O(6)	0.0060	0.0103	0.0170	0.0258	0.0360
O(7)	-0.0081	-0.0081	-0.0079	-0.0074	-0.0068
O(8)	-0.0087	-0.0087	-0.0085	-0.0082	-0.0079
O(9)	-0.0081	-0.0081	-0.0079	-0.0074	-0.0068
O(10)	-0.0087	-0.0087	-0.0085	-0.0082	-0.0079
Cl(11)	0.0165	0.0149	0.0129	0.0107	0.0086
Cl(12)	0.0252	0.0236	0.0216	0.0196	0.0177
Cl(13)	0.0165	0.0149	0.0129	0.0107	0.0086
Cl(14)	0.0252	0.0236	0.0216	0.0196	0.0177
C(15)	0.0044	0.0061	0.0073	0.0078	0.0075
C(16)	0.0044	0.0061	0.0073	0.0078	0.0075

Cr(3) and Cr(4), respectively, and the terminal Cl(13) and Cl(14) atoms have  $\alpha$  spin populations due to the spin delocalization from the Cr(3) center and the Cl(11) and Cl(12) have  $\beta$  spin populations due to the spin delocalization from the Cr(4) center. Thus the spin population analysis for the BS state further confirms the magnetic exchange mechanisms deduced from the HS state. In connection with the superexchange pathway of this compound it should be pointed out that though the spin delocalization occurs between the Cr and the bridging methoxy oxygen atoms, there is a spin polarization interaction between the Cr and the axial bridge oxygen. The magnetic exchange coupling between the Cr(III) centers can be mediated by the methoxy oxygen and the more extended O-C-C-C-O network (see Figure 1a). We suspect that the latter pathway is an inefficient route for the enhanced magnetic communication between Cr(III) ions, because the spin polarization mechanism may cause the weak magnetic exchange interaction between the two Cr(III) centers.

The dependence of the spin populations on Cr(III) centers on the Cr-O-Cr bridging angle ranging from 82.8° to 106.9° for the model compound in the high-spin state is shown in Table 6. From Table 6 the unpaired electrons of magnetic Cr(III) ions are partially delocalized to bridging oxygen atoms. This leads to smaller spin populations on the chromium ions and larger spin populations on the two bridging oxygen atoms with smaller Cr-O-Cr angles. This result can be easily rationalized using the theory of Kahn and Briat.<sup>22</sup> The reinforcement of antiferromagnetic interactions on decreasing the bridging angle implies the increase of delocalization of the unpaired electrons on magnetic centers toward bridging ligands and hence the decrease of the spin populations on Cr(III) ions. Obviously, spin density distributions through bridging methoxy groups are in agreement with the prediction of spin delocalization model.

### Conclusions

We have investigated the effect of the different bridging angles of core arrangements on the exchange coupling in the  $[\text{Cr}_2(\text{OCH}_3)_2(\text{H}_2\text{O})_4\text{Cl}_4]$  model compound and the magneto-structural correlations corresponding to the bridging angle distortion for this family of compounds. Qualitative orbital model proposed by Hoffmann et al. is useful in analyzing the results, giving good estimates for the antiferromagnetic contribution to the exchange coupling in this family of compounds. From our results we find that the  $-J$  values increase with decreasing bridging angles in the range 83–101°. A very strong antiferromagnetic coupling found for structures that present small Cr–O–Cr angles is related to the important  $\sigma$  overlap between the  $x^2-y^2$  metal orbitals. It can be concluded that the contribution from the  $x^2-y^2$  magnetic orbitals is responsible for the correlation between the coupling constant  $J$  and the bridging angle and the antiferromagnetic coupling through methoxy groups is mainly due to spin delocalization effect.

**Acknowledgments.** This work was supported by the Kyungshung University Research Grant in 2008.

### References

1. Kahn, O. *Molecular Magnetism*. VCH Publishers: New York, 1993.
2. Nagao, H.; Nishino, M.; Shigeta, Y.; Soda, T.; Kitagawa, Y.; Onishi, T.; Yoshioka, Y.; Yamaguchi, K. *Coord. Chem. Rev.* **2000**, *198*, 265.
3. Noodleman, L. *J. Chem. Phys.* **1981**, *74*, 5737.
4. (a) Ruiz, E.; Alemany, P.; Alvarez, S.; Cano, J. *Inorg. Chem.* **1997**, *36*, 3683. (b) Ruiz, E.; Alemany, P.; Alvarez, S.; Cano, J. *J. Am. Chem. Soc.* **1997**, *119*, 1297.
5. (a) Ruiz, E.; Cano, J.; Alvarez, S.; Alemany, P. *J. Comput. Chem.* **1999**, *20*, 1391. (b) Ruiz, E.; Alvarez, S.; Rodriguez-Fortea, A.; Alemany, P.; Pouillon, Y.; Massobrio, C. In *Magnetism: Molecules to Materials*; Miller, J. S.; Drillon, M., Eds.; Wiley-VCH: Weinheim, 2001; pp 227–279. (c) Cano, J.; Rodriguez-Fortea, A.; Alemany, P.; Alvarez, S.; Ruiz, E. *Chem. Eur. J.* **2000**, *6*, 327.
6. Becke, A. D. *J. Chem. Phys.* **1993**, *98*, 5648.
7. Frisch, M. J.; Trucks, G. W.; Schlegel, H. B.; Scuseria, G. E.; Robb, M. A.; Cheeseman, J. R.; Zakrzewski, V. G.; Montgomery, J. A.; Stratmann, R. E.; Burant, J. C.; Dapprich, S.; Millam, J. M.; Daniels, A. D.; Kudin, K. N.; Strain, M. C.; Farkas, O.; Tomasi, J.; Barone, V.; Cossi, M.; Cammi, R.; Mennucci, B.; Pomelli, C.; Adamo, C.; Clifford, S.; Ochterski, J.; Petersson, G. A.; Ayala, P. Y.; Cui, Q.; Morokuma, K.; Malick, D. K.; Rabuck, A. D.; Raghavachari, K.; Foresman, J. B.; Cioslowski, J.; Ortiz, J. V.; Stefanov, B. B.; Liu, G.; Liashenko, A.; Piskorz, P.; Komaromi, I.; Gomperts, R.; Martin, R. L.; Fox, D. J.; Keith, T.; Al-Laham, M. A.; Peng, C. Y.; Nanayakkara, A.; Gonzalez, C.; Challacombe, M.; Gill, P. M. W.; Johnson, B. G.; Chen, W.; Wong, M. W.; Andres, J. L.; Head-Gordon, M.; Replogle, E. S.; Pople, J. A. *Gaussian 03, Revision C.02*; Gaussian, Inc.: Pittsburgh, PA, 2003.
8. Becke, A. D. *Phys. Rev. A* **1988**, *38*, 3098.
9. Lee, C.; Yang, W.; Parr, R. G. *Phys. Rev. B* **1988**, *37*, 785.
10. Schaefer, A.; Horn, H.; Ahlrichs, R. *J. Chem. Phys.* **1992**, *97*, 2571.
11. Schaefer, A.; Huber, C.; Ahlrichs, R. *J. Chem. Phys.* **1994**, *100*, 5829.
12. Talbot-Eeckelaers, C. E.; Rajaraman, G.; Cano, J.; Aromi, G.; Ruiz, E.; Brechin, E. K. *Eur. J. Inorg. Chem.* **2006**, 3382.
13. Hodgson, D. J. In *Magneto-Structural Correlations in Exchange Coupled Systems*, NATO ASI Series C; Willet, R. D.; Gatteschi, D.; Kahn, O., Eds.; Dordrecht: 1985; p 497.
14. Hay, P. J.; Thibault, J. C.; Hoffmann, R. *J. Am. Chem. Soc.* **1975**, *97*, 4884.
15. (a) Kang, D. B. *Bull. Korean Chem. Soc.* **2005**, *26*, 1965. (b) Bae, H. W.; Koo, H.-J. *Bull. Korean Chem. Soc.* **2008**, *29*, 122.
16. Desplanches, C.; Ruiz, E.; Rodriguez-Fortea, A.; Alvarez, S. *J. Am. Chem. Soc.* **2002**, *124*, 5197.
17. Whangbo, M.-H.; Koo, H.-J.; Dai, D. *J. Solid State Chem.* **2003**, *176*, 417.
18. Estes, E. D.; Scaringe, R. P.; Hatfield, W. E.; Hodgson, D. J. *Inorg. Chem.* **1976**, *15*, 1179.
19. Fischer, H. R.; Hodgson, D. J.; Pedersen, E. *Inorg. Chem.* **1984**, *23*, 4755.
20. Clerac, R.; Cotton, F. A.; Murillo, C. A.; Wang, X. P. *Chem. Commun.* **2001**, 205.
21. Paine, T. K.; Weyhermuller, T.; Wieghardt, K.; Chaudhuri, P. *Inorg. Chem.* **2002**, *41*, 6538.
22. (a) Kahn, O.; Briat, B. *J. Chem. Soc. Faraday Trans.* **1976**, *72*, 268. (b) Girerd, J. J.; Journaux, Y.; Kahn, O. *Chem. Phys. Lett.* **1981**, *82*, 534.